

Metal-insulator transition in $\text{NiS}_{2-x}\text{Se}_x$

J. Kuneš,^{1,2} L. Baldassarre,³ B. Schächner,³ C. A. Kuntscher,³ Dm. M. Korotin,⁴ and V. I. Anisimov⁴

¹*Theoretical Physics III, Center for Electronic Correlations and Magnetism,
Institute of Physics, University of Augsburg, Augsburg 86135, Germany**

²*Institute of Physics, Academy of Sciences of the Czech Republic,
Čukrovarnická 10, 162 53 Praha 6, Czech Republic*

³*Experimental Physics II, Institute of Physics, University of Augsburg, Augsburg 86135, Germany*

⁴*Institute of Metal Physics, Russian Academy of Sciences-Ural Division, 620041 Yekaterinburg GSP-170, Russia*

(Dated: February 6, 2020)

Using a combination of first-principles bandstructure and dynamical mean-field approximation with a quantum Monte-Carlo impurity solver we study the single-particle spectra of NiS_2 and NiSe_2 . We identify the hybridization splitting within the S-S (Se-Se) dimer to be the main parameter controlling the appearance of the charge gap. Implications for the metal-insulator transition in $\text{NiS}_{2-x}\text{Se}_x$ driven by external pressure or increasing Se content are discussed and confronted with new optical data.

PACS numbers: 71.30.+h, 62.50.-p, 78.30.-j

The metal-insulator transition (MIT) driven by electronic correlations has been subject of intense research for several decades. The $\text{NiS}_{2-x}\text{Se}_x$ series provided an important model system exhibiting a MIT controlled by varying the Se content x , temperature T or pressure P [1, 2, 3, 4, 5]. Particularly interesting is the similarity of its $x - T$ [2, 3] and $P - T$ phase diagrams [4] to that of the Hubbard model in the infinite dimensional limit [6]. Consequently, the MIT has been commonly attributed to broadening of the Ni- d band [3, 4, 5, 7, 8, 9]. Despite a large volume of available experimental data the microscopic origin of the MIT in $\text{NiS}_{2-x}\text{Se}_x$ is poorly understood and a satisfactory material-specific theory is missing. Trying to provide such a theory we uncover an unexpected microscopic control parameter and mechanism governing the physics of $\text{NiS}_{2-x}\text{Se}_x$.

The electronic structure of NiX_2 ($X=\text{S,Se}$) is investigated using a combination of the *ab initio* bandstructure and the approximation of the dynamical mean-field theory (LDA+DMFT) [6, 10], supplemented by infrared (IR) reflectivity measurements under pressure. We address the questions: i) Why is NiS_2 an insulator and NiSe_2 a metal? ii) How do NiX_2 respond to external pressure, and are the effects of pressure and varying Se content equivalent?, iii) What is the mechanism of the MIT in $\text{NiS}_{2-x}\text{Se}_x$?

NiX_2 can be viewed as NiO with the O atom replaced by an X_2 dimer, which accommodates two holes in its p_σ^* anti-bonding orbitals leading to an X_2^{-2} valence state. Numerous photoemission (PES) studies [7, 11, 12] complemented by cluster calculations [7] revealed a similarity between the NiX_2 and NiO valence band (VB) spectra, supporting this analogy. The bandstructure calculations in the local density approximation (LDA) [8, 13, 14] rendered NiS_2 a metal with a partially filled e_g band and empty p_σ^* orbitals. By analogy to NiO it was speculated that local $d - d$ correlations open a gap between

the S- p band and the upper Hubbard band of Ni- d e_g character [8], leading to the classification of NiS_2 as a charge-transfer (CT) insulator in the Zaanen-Sawatzky-Allen (ZSA) scheme [15].

Our computations proceed as follows. First, we perform paramagnetic LDA calculations [16] and find the equilibrium S(Se) positions. Second, we represent the one-particle Hilbert space of the hybridized Ni- d and S(Se)- p bands in Wannier basis (44 orbitals per unit cell) and calculate the parameters of the on-site $d - d$ interaction with the constraint LDA approach [17, 18]. We found only moderately different $U_{\text{NiS}_2} = 5$ eV and $U_{\text{NiSe}_2} = 4.7$ eV and used J of 1 eV throughout the study. Third, we use the Hamiltonian from the previous step, augmented by the local interaction and self-consistently corrected for the double-counting [19], and solve the DMFT equations using the continuous time quantum Monte-Carlo impurity solver [20] and the maximum entropy method [21] to calculate the single-particle spectral densities.

In Fig. 1 we show the calculated NiS_2 spectra, which exhibit a small charge gap in agreement with experimental observations. The valence band spectrum resembles that of NiO [22] with the distribution of spectral weight between d^7 (lower Hubbard band around -6 eV) and $d^8 \underline{L}$ final states at low binding energy, a result of a strong $p - e_g$ hybridization. The experimental VB spectrum, obtained by x-ray photoemission spectroscopy (XPS), exhibits several pronounced features which find their theoretical counterparts. Particularly important for the further discussion is the high-energy shoulder at -8 eV, dominated by S- p density with a large p_σ contribution in agreement with the observation of Ref. 11.

The comparison of the conduction band (CB) spectrum to the experimental data from Bremsstrahlung isochromat spectroscopy (BIS) is less straightforward. The key question for understanding the physics of NiX_2

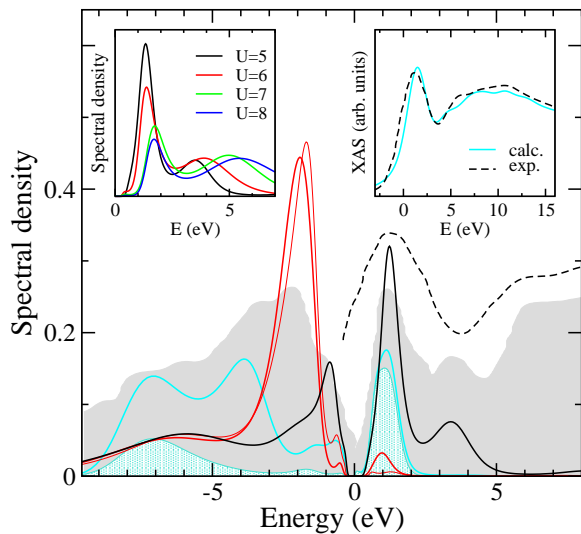


FIG. 1: (color online) The calculated ($U=5$ eV, $T=580$ K) orbitally resolved spectra of NiS_2 [$\text{Ni-d}:e_g^\sigma$ (black) and $t_{2g}=e_g^\pi$ (thick red) + a_{1g} (thin red); S- p : total (blue) and p_σ (blue-shaded)] compared to the experimental XPS+BIS (gray, shaded) [12] and S K-edge XAS (dashed) [23] spectra. The left inset shows the conduction band e_g^σ spectra for $U=5, 6, 7,$ and 8 eV. In the right inset the experimental (dashed) and calculated (blue) S K-edge XAS spectra are compared.

is the relative position of the upper Hubbard band and the p_σ^* band. The experimental BIS spectrum exhibits three distinct features: a sharp low-energy peak at 1 eV, a high-energy peak at 3.5 eV and a broad band starting around 5.5 eV. The authors of Ref. 12 interpreted the 1 eV as Ni- d upper Hubbard band and the 3.5 eV peak as S p_σ^* band. Our results provide a different picture, we identify the p_σ^* with the 1 eV peak and the upper Hubbard band with the 3.5 eV peak. (By construction, there is no contribution of our Wannier states to the broad band.) A sizable d contribution to the low energy peak at 1 eV corresponds to the $t_{2g}^5 e_g^3 p_\sigma^*$ final state, reached by $t_{2g} - p_\sigma^*$ electron transfer.

Our results are supported by x-ray absorption (XAS) measurements at the S K edge which probe the empty S- p states [23]. Taking into account the high-energy broad band and the dipole transition amplitudes obtained from the LDA calculation [16] we find a good agreement with the experimental spectra shown in the right inset of Fig. 1. Lacking the S- p character the 3.5 eV peak does not contribute to the XAS spectrum.

Further insight into the nature of the CB can be gained by varying the interaction strength U as shown in the left inset of Fig. 1. As expected, the upper Hubbard band moves towards higher energies with increasing U , while the resonant low-energy peak loses some intensity and moves slightly with respect to the p_σ^* band. The spectra exhibit only a minor temperature dependence in the studied range 290-1160 K.

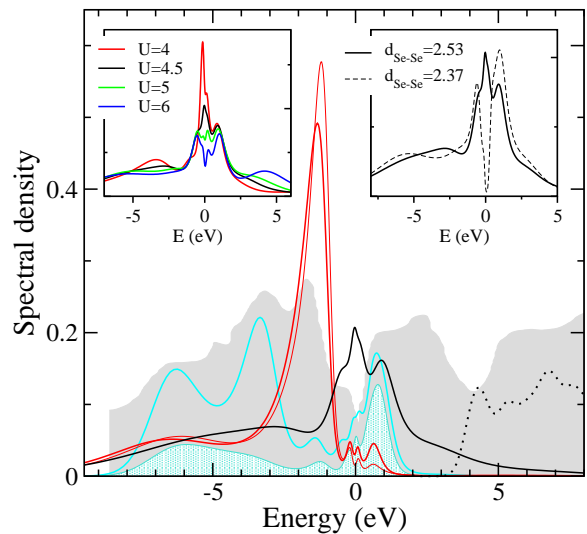


FIG. 2: (color online) The calculated ($U=4.5$ eV, $T=580$ K) orbital resolved spectra of NiSe_2 compared to the experimental XPS+BIS [12] spectra. (the same notation as in Fig. 1) The left inset shows the e_g^σ densities for various interaction strengths U (eV). In the right inset the effect of reducing the Se-Se distance (\AA) on e_g^σ spectra ($U=4.5$ eV) is shown.

The VB spectra of NiSe_2 (Fig. 2) overall resemble the NiS_2 ones with some quantitative differences, such as the shift of the high-energy shoulder to -6.5 eV, also visible in the experimental data. However, NiSe_2 turns out to be metallic. Its low-energy spectrum is rather sensitive to changes of U , as shown in the left inset of Fig. 2. For $U < 5$ eV, a temperature-dependent peak appears at the chemical potential. The spectrum remains gapless up to the largest studied value of $U=8$ eV (not shown). As in NiS_2 we find the p_σ^* band at the bottom of the CB manifold. Since the splitting between the VB bottom and the p_σ^* peak is essentially a molecular property of the Se-Se dimer it does not depend on the value of U .

To analyze the role of the p_σ^* band we calculate the bare S(Se)- p bandstructures, obtained by decoupling the Ni- d states. This is done conveniently by removing the Ni-centered orbitals from the LDA basis set [Fig. 3(c),(d)], or rigorously using the $p-p$ block of the Hamiltonian in Wannier basis [Fig. 3(a),(b)] with similar results. The key difference between NiS_2 and NiSe_2 is the size of the gap separating the p_σ^* band from the rest of the p -manifold. As demonstrated in Fig. 3(c) the gap is controlled by the length of the S(Se) dimer. Fig. 3(e) shows the LDA inter-atomic distances as a function of the lattice constant. The experimental and theoretical data for NiS_2 agree very well with each other. The rigidity of the S-S dimer underlines its molecular character. Surprisingly, the computed Se-Se distance overestimates the experimental one by about 5%. To assess the effect of this variance a calculation with a reduced Se-Se distance [dashed bands in Fig. 3(c)] of 2.37 \AA (just below the ex-

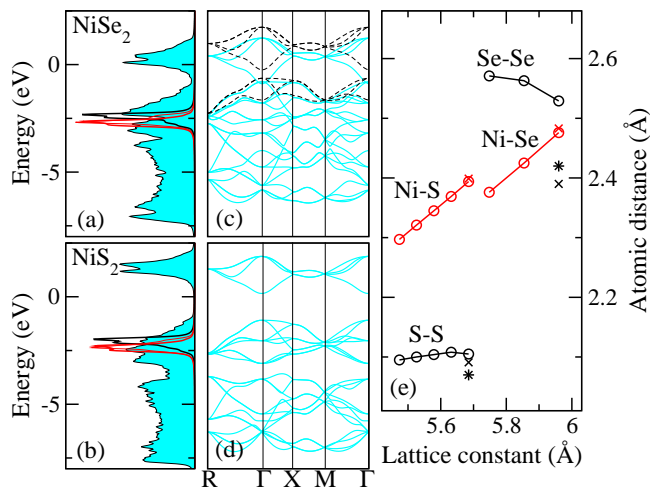


FIG. 3: (color online) The bare S(Se)- p spectral densities and bandstructures. The spectral densities in the left panel [(a),(b)] are obtained from a Wannier function Hamiltonian, while the bandstructures in the middle panel [(c),(d)] are based on a LAPW calculation with removed Ni-like basis functions. Dashed bands for NiSe₂ correspond to a reduced Se-Se distance. The right panel (e) shows the calculated pressure dependence of the inter-atomic distances. The isolated points mark the experimental values of Refs. 12 (star) and 24 (cross).

perimental values) was carried out. An increase of the bonding – anti-bonding splitting leads to a strong suppression of the spectral density at the lowest energies (see the right inset of Fig. 2), but is not sufficient to open a charge gap.

The DMFT calculations for NiS₂ at pressures up to 13 GPa were performed and the closing of the charge gap was observed. We defer the details and the results for optical and transport properties to a separate publication and discuss the general aspects of applied pressure. As suggested by the rigidity of the S-S dimer, the bonding – anti-bonding splitting is insensitive to pressure. On the other hand, the widths of the individual p -bands, controlled by the inter-dimer distances, increase with pressure. This leads to a reduction of the bare p -gap, and the p_{σ}^* band eventually starts to overlap the Ni- e_g dominated top of the VB rendering the material metallic. The LDA data show that, compared to S-S, the Se-Se dimers are more sensitive to moderate pressures, which reduce the bonding – anti-bonding splitting along with an increase of the Se-Se distance. Therefore the pressure-induced closing of the charge gap is expected to proceed faster in compounds with higher Se content.

To verify this conclusion and to obtain further information about the electronic properties of NiS_{2-x}Se_x we have measured the pressure-dependent reflectivity at near-normal incidence on high quality single crystals grown by a vapor transport technique using an IR microscope coupled to a Michelson interferometer. A clamp diamond anvil cell (Diacell cryoDAC-Mega) equipped with type

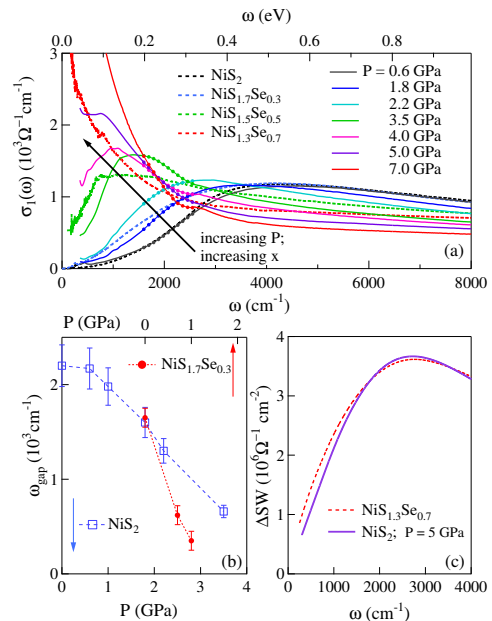


FIG. 4: (color online) (a) Room-temperature optical conductivity spectra of NiS_{2-x}Se_x ($x \geq 0.3$) at ambient pressure compared with those of NiS₂ at elevated pressures. (b) The gap vs pressure for NiS₂ and NiS_{1.7}Se_{0.3} (note the mutual horizontal offset) (c) SW transfer ΔSW for NiS₂ at 5 GPa and for NiS_{1.3}Se_{0.7} at ambient pressure.

IIa diamonds was employed. The measurement procedure, as well as the data processing to extract the optical conductivity $\sigma_1(\omega)$ are described in Refs. 25, 26. The optical conductivities at ambient conditions for the NiS_{2-x}Se_x series ($x=0; 0.3; 0.5; 0.7$) and at various pressures (up to 7 GPa) for NiS₂ are shown in Fig. 4(a).

A well-defined gap followed by an absorption band is found for NiS₂. As Se is introduced, or as pressure is applied, the absorption band moves towards lower energies, progressively closing the gap. We define the experimental gap as the frequency at half-height of the absorption band. This definition of the gap leads to a similar pressure dependence as obtained by linearly extrapolating the steepest rise of $\sigma_1(\omega)$ [27] or by considering the maximum of the absorption peak obtained with Drude-Lorentz fitting [28]. Comparing the corresponding conductivity spectra we find that pressure on NiS₂ and S substitution by Se have a qualitatively similar effect following the scaling $P[\text{GPa}] \approx x/0.15$ of Ref. 5.

In Fig. 4(b) we compare the pressure dependence of the optical gaps for pure NiS₂ and NiS_{1.7}Se_{0.3} (horizontally off-set according to the scaling relation). We find that in the Se-doped compound pressure is more efficient in closing the gap, in accord with the above theoretical reasoning. Next we discuss the metallic phase. To quantify the 'metallicity' we use the spectral weight (SW) transfer relative to the ambient pres-

sure NiS₂ data $\Delta SW = SW(x, P) - SW(x=0, P=0)$, where $SW(\omega) = \int_0^\omega \sigma_1(\omega') d\omega'$. Like recent IR measurements [13], our data can be fitted with two distinct features: a Drude-like term and a Lorentz peak in the mid-IR region. With applied pressure a large part of the spectral weight is transferred to the mid-IR region first, followed by appearance of Drude-like peak upon further pressure increase [see Fig. 4(a)]. Without making a quantitative connection we point out that a qualitatively similar behavior is observed in the DMFT results when the Se-Se distance is varied (right inset of Fig. 2). Following the scaling relation we compare NiS₂ at 5 GPa with NiS_{1.3}Se_{0.7} at ambient pressure in Fig. 4. Although a similar amount of SW is transferred below 4000 cm⁻¹, NiS_{1.3}Se_{0.7} exhibits a higher SW transfer at lower frequencies (<2000 cm⁻¹) pointing to a more intense Drude-like term. This observation also supports our conclusion about the faster onset of metallicity in Se-rich samples.

In conclusion, using the LDA+DMFT approach we have reproduced the groundstates of NiS₂ (insulator) and NiSe₂ (metal) and provide the following answers to the questions posed in the introduction: i) The different groundstates of NiS₂ and NiSe₂ are consequence of a larger gap in the bare *p*-bandstructure (*p*-gap) of NiS₂ resulting from stronger bonding within the S-S dimer. ii) The pressure reduces the *p*-gap by broadening the individual *p*-bands, while the Se substitution reduces the *p*-gap due to smaller bonding-anti-bonding splitting. iii) The MIT is controlled by varying the size of the *p*-gap. We find both computationally and experimentally that the pressure driven MIT is accelerated by the Se substitution. The conceptual picture of NiS_{2-x}Se_x is provided by a periodic Anderson model with a variable gap in the conduction electron bath rather than the charge-transfer insulator model.

We thank P. Werner for providing his quantum Monte-Carlo code and D. Vollhardt for critical reading of the manuscript. L.B. and C.A.K. thank B. Gasharova, Y.-L. Mathis, D. Moss, and M. Süpfle for help at the IR beamline and H. Takagi for kindly providing the samples. We acknowledge the financial support of SFB 484 of the Deutsche Forschungsgemeinschaft (J.K., L.B., C.A.K.), Fondazione della Riccia and Bayerische Forschungsförderung (L.B.), and Russian Foundation for Basic Research under Grant No. RFFI-07-02-00041, Dynasty Foundation, President of Russian Federation fund NSH 1941.2008.2 and Program of Russian Academy of Science Presidium “Quantum microphysics of condensed matter” N7 (Dm.M.K, V.I.A.), beam time provided by ANKA Angströmquelle Karlsruhe and computertime provided by Leibniz Supercomputing Center Munich.

-
- * Electronic address: jan.kunes@physik.uni-augsburg.de
- [1] P. Kwizera, M. S. Dresselhaus, and D. Adler, Phys. Rev. B **21**, 2328 (1980).
 - [2] X. Yao, J. M. Honig, T. Hogan, C. Kannewurf, and J. Spalek, Phys. Rev. B **54**, 17469 (1996).
 - [3] M. Matsuura, H. Hiraka, K. Yamada, and Y. Endoh, J. Phys. Soc. Jpn. **69**, 1503 (2000).
 - [4] N. Takeshita, S. Takashima, C. Terakura, H. Nishikubo, S. Miyasaka, M. Nohara, Y. Tokura, and H. Takagi, arXiv:0704.0591.
 - [5] S. Miyasaka, H. Takagi, Y. Sekine, H. Takahashi, N. Mori, and R. J. Cava, J. Phys. Soc. Jpn. **69**, 3166 (2000).
 - [6] A. Georges, G. Kotliar, W. Krauth, and M. J. Rozenberg, Rev. Mod. Phys. **68**, 13 (1996).
 - [7] A. Fujimori, K. Mamiya, T. Mizokawa, T. Miyadai, T. Sekiguchi, H. Takahashi, N. Mori, and S. Suga, Phys. Rev. B **54**, 16329 (1996); S. R. Krishnakumar and D. D. Sarma, Phys. Rev. B **68**, 155110 (2003).
 - [8] A. Y. Matsuura, Z. X. Shen, D. S. Dessau, C. H. Park, T. Thio, J. W. Bennett, and O. Jepsen, Phys. Rev. B **53**, R7584 (1996).
 - [9] D. D. Sarma, M. Pedio, M. Capozzi, A. Girycki, N. Chandrasekharan, N. Shanthi, S. R. Krishnakumar, C. Ottaviani, C. Quaresima, and P. Perfetti, Phys. Rev. B **57**, 6984 (1998).
 - [10] K. Held, I. A. Nekrasov, G. Keller, V. Eyert, N. Blümer, A. K. McMahan, R. T. Scalettar, T. Pruschke, V. I. Anisimov, and D. Vollhardt, phys. stat. sol. (b) **243**, 2599 (2006); G. Kotliar, S. Y. Savrasov, K. Haule, V. S. Oudovenko, O. Parcollet, and C. A. Marianetti, Rev. Mod. Phys. **78**, 865 (2006).
 - [11] E. K. Li, K. H. Johnson, D. E. Eastman, and J. L. Freeouf, Phys. Rev. Lett. **32**, 470 (1974).
 - [12] W. Folkerts, G. A. Sawatzky, C. Haas, R. A. de Groot, and F. U. Hillebrecht, J. Phys. C **20**, 4135 (1987).
 - [13] A. Perucchi, C. Marini, M. Valentini, P. Postorino, R. Soprocase, P. Dore, P. Hansmann, O. Jepsen, G. Sangiovanni, A. Toschi, et al., arXiv:0811.2154.
 - [14] D. W. Bullett, J. Phys. C **15**, 6163 (1982).
 - [15] J. Zaanen, G. A. Sawatzky, and J. W. Allen, Phys. Rev. Lett. **55**, 418 (1985).
 - [16] P. Blaha, K. Schwarz, G. K. H. Madsen, D. Kvasnicka, and J. Luitz, *WIEN2K, An Augmented Plane Wave + Local Program for Calculating Crystal Properties* (Technical University Wien, Austria, 2001).
 - [17] D. M. Korotin, A. V. Kozhevnikov, S. L. Skornyakov, I. Leonov, N. Binggeli, V. I. Anisimov, and G. Trimarchi, Eur. Phys. J **65**, 91 (2008).
 - [18] S. Baroni, A. D. Corso, S. de Gironcoli, P. Giannozzi, C. Favazzoni, G. Ballabio, S. Scandolo, G. Chiarotti, P. Focher, A. Pasquarello, et al., <http://www.pwscf.org/>.
 - [19] J. Kuneš, Dm. M. Korotin, M. A. Korotin, V. I. Anisimov, and P. Werner, Phys. Rev. Lett. **102**, 146402 (2009).
 - [20] P. Werner, A. Comanac, L. de Medici, M. Troyer, and A. J. Millis, Phys. Rev. Lett. **97**, 076405 (2006).
 - [21] M. Jarrell and J. E. Gubernatis, Phys. Rep. **269**, 133 (1996).
 - [22] J. Kuneš, V. I. Anisimov, A. V. Lukoyanov, and D. Vollhardt, Phys. Rev. B **75**, 165115 (2007).

- [23] C. Sugiura and S. Muramatsu, *phys. stat. sol. (b)* **129**, K157 (1985).
- [24] R. Otero, J. L. M. deVidales, and C. de las Heras, *J. Phys.: Condens. Matter* **10**, 6919 (1998).
- [25] A. Pashkin, M. Dressel, and C. A. Kuntscher, *Phys. Rev. B* **74**, 165118 (2006).
- [26] L. Baldassarre, A. Perucchi, E. Arcangeletti, D. Nicoletti, D. Di Castro, P. Postorino, V. A. Sidorov, and S. Lupi, *Phys. Rev. B* **75**, 245108 (2007).
- [27] T. Katsufuji, Y. Okimoto, and Y. Tokura, *Phys. Rev. Lett.* **75**, 3497 (1995).
- [28] F. Wooten, *Optical properties of solids* (Academic Press, New York, 1972).